International Geology Review
Publication details, including instructions for authors and subscription information:
http://www.tandfonline.com/loi/tigr20

Trace element geochemistry of the Mt Vulture carbonatites, southern Italy

Giovanni Mongelli [a b], Michele Paternoster [a], Giovanna Rizzo [a], Maria T. Cristi Sansone [a] & Rosa Sinisi [c]

[a] Department of Sciences, University of Basilicata, 85100, Potenza, Italy

[b] National Research Council - Institute of Methodologies for Environmental Analysis, 85050, Tito Scalo, PZ, Italy

[c] Department of Nature and Earth Sciences, University of Sassari, 07100, Sassari, Italy

Version of record first published: 05 Apr 2013.

To cite this article: Giovanni Mongelli , Michele Paternoster , Giovanna Rizzo , Maria T. Cristi Sansone & Rosa Sinisi (2013): Trace element geochemistry of the Mt Vulture carbonatites, southern Italy, International Geology Review, DOI:10.1080/00206814.2013.786310

To link to this article: http://dx.doi.org/10.1080/00206814.2013.786310

International Geology Review, 2013
http://dx.doi.org/10.1080/00206814.2013.786310

Taylor & Francis
Taylor & Francis Group

Trace element geochemistry of the Mt Vulture carbonatites, southern Italy

Giovanni Mongelli[a,b], Michele Paternoster[a], Giovanna Rizzo[a]*, Maria T. Cristi Sansone[a] and Rosa Sinisi[c]

[a]*Department of Sciences, University of Basilicata, 85100 Potenza, Italy;* [b]*National Research Council – Institute of Methodologies for Environmental Analysis, 85050 Tito Scalo (PZ), Italy;* [c]*Department of Nature and Earth Sciences, University of Sassari, 07100 Sassari, Italy*

(*Accepted 11 March 2013*)

The Mt Vulture carbonatites are the only carbonatite occurrence in the southern Apennines. We present new trace element data for these rocks in order to evaluate the factors influencing rare earth element (REE) and other trace element fractionations and their REE grade. This study focuses on massive hyalo-alvikites from two lava flows and one dike, which have different relative abundances of silicate and carbonate (i.e. Si/Ca). These differences are also evident from CaO/(CaO + MgO + FeO(T) + MnO) and Sr/Ba ratios. The REE grade of the Mt Vulture carbonatites is very similar to that of the global average for calcio-carbonatites. R-mode factor analysis shows that most of the trace element variance reflects the relative roles of carbonate and silicate minerals in influencing trace element distributions. Silicates largely control heavy rare earth element (HREE), transition metal, Zr, and Th abundances, whereas carbonate minerals control light rare earth element (LREE), Ba, and Pb abundances. In addition, apatite influences LREE concentrations. Increasing silica contents are accompanied by decreases in (La/Yb)N and (La/Sm)N ratios and less marked LREE enrichment. In contrast, higher carbonate contents are associated with increases in (La/Yb)N and (La/Sm)N. The Si/Ca ratio has little influence on Eu anomalies and middle rare earth element (MREE) to HREE fractionations. Apatite has a negligible effect on inter-REE fractionations amongst the carbonatites.

Keywords: carbonatites; Mt Vulture; REE fractionation; R-mode factor analysis; ore geochemistry

Introduction

Carbonatites are igneous rocks comprising >50 modal% magmatic carbonate and >20 wt.% SiO_2 (Le Maitre 2002). The origins of carbonatite magmas are debated, and models proposed for carbonatite generation include (1) melting of a carbonate-bearing mantle source (e.g. Sweeney 1994; Harmer and Gitiins 1998; Srivastava *et al*. 2005), (2) immiscible liquids from CO_2-rich silicate magmas (e.g. Koster van Groos and Wyllie 1963; Kjarsgaard and Hamilton 1989), and (3) extensive crystal fractionation from CO_2-rich silicate magmas (e.g. Lee and Wyllie 1994; Veksler *et al*. 1998).

Carbonatite ages range from Archaean to recent and these rocks chiefly occur in continental regions, although a few have been reported in oceanic settings (e.g. Bell 1998). Most carbonatites occupy rifting environments, but some occur in orogenic belts (Xu *et al*. 2010, and references therein). Continental carbonatites are typically associated with alkaline igneous rocks. The study of these carbonatites and their associated alkaline rocks can provide insights into mantle and crustal processes, including melt extraction, recycling of crustal material, mantle metasomatism, mantle degassing, and silicate–carbonate immiscibility, as well the secular evolution of the mantle (e.g. Ray *et al*. 2000, and references therein).

Carbonatites also contain the highest concentrations of rare earth elements (REEs) of any igneous rock type, an important feature considering the rapid rise in world demand for these elements and concerns about their future availability (Tucker *et al*. 2012). Furthermore, ores of Cu, Nb, Mo, fluorite, phosphate, and vermiculite are associated with carbonatites (Xu *et al*. 2010).

In southern Italy, carbonatites are present only in the Mt Vulture area, where previous petrological and geodynamical studies have yielded contrasting views of their origin (e.g. Stoppa and Principe 1997; D'Orazio *et al*. 2007; Rosatelli *et al*. 2007; Stoppa *et al*. 2008). These earlier studies have largely presented mineral chemistry and whole-rock trace element, and isotopic data for the carbonatites (D'Orazio *et al*. 2007; Rosatelli *et al*. 2007), although the data presently available for these rocks are sparse. Accordingly, we present new chemical data for a suite of carbonatite rocks from the Mt Vulture area and use these data to discuss the relationships between carbonatite occurrence and REE distribution. In particular, we focus on the factors affecting REE fractionations, which may

*Corresponding author. Email: giovanna.rizzo@unibas.it

be useful for future REE exploration in similar geological settings worldwide.

Geological setting

Mt Vulture is a Pleistocene composite volcano located at the easternmost border of the Apennine Mountains at the western margin of the Apulia foreland (Figure 1). The volcanic rocks cover an area of approximately 150 km^2 and are the result of both explosive and effusive activity that took place from the middle to upper Pleistocene (Serri *et al*. 2001). Compared with other major Quaternary volcanoes of Italy that are scattered along the Tyrrhenian margin, Mt Vulture is the only volcano located to the east of the Apennine chain on an along-dip vertical slab window (Doglioni *et al*. 1994; D'Orazio *et al*. 2007; Caracausi *et al*. 2013). Beccaluva *et al*. (2002) suggested that the magmas of Mt Vulture were generated from lithospheric mantle and were enriched in an alkaline silicate–carbonatite anorogenic component, as well as being affected by subduction-related potassic metasomatism. Downes *et al*. (2002) used trace element data to show that the lithosphere beneath Mt Vulture had already undergone extensive partial melting before experiencing subduction-related silicate melt metasomatism. However, D'Orazio *et al*. (2007) proposed that the Mt Vulture magmas were derived from a hybrid mantle that originated from the interaction between Adriatic mantle and metasomatized mantle wedge material flowing eastwards from the Campanian–Tyrrhenian region due to a vertical tear in the retreating Adriatic lithospheric slab. Therefore, the mantle source of Mt Vulture magmas may comprise variable contributions from intra-plate and subduction-related components.

Volcanic activity at Mt Vulture started at 742 ± 11 ka and continued until 142 ± 11 ka, although this interval was characterized by a number of quiescent periods (Büettner *et al*. 2006, and references therein). The volcanic rocks are strongly silica-undersaturated and have alkaline potassic to ultrapotassic affinities (De Fino *et al*. 1986). Giannandrea *et al*. (2006a) grouped the volcanic units into two distinct super-synthems: the Mt Vulture and Monticchio phases. The Mt Vulture units are the oldest volcanic products and comprise lavas and pyroclastic deposits that range in composition from basanite-foidite to phonolite. The Monticchio units were produced by monogenetic eruptions of tectonically controlled volcanic vents (Giannandrea *et al*. 2006b) and comprise an unusual combination of mantle xenoliths, melilite, and carbonatite juvenile rock fragments within carbonatitic–melilitic tuffs (Stoppa and Principe 1997; Jones *et al*. 2000; Downes *et al*. 2002).

The carbonatites studied in this article are part of the sequence erupted from a small volcanic centre on the northern slope of Mt Vulture whose origin is debated (e.g. D'Orazio *et al*. 2007, 2008; Stoppa *et al*. 2008). Giannandrea *et al*. (2004) identified this sequence as the Imbandina Subsynthem, which mostly comprises massive deposits of ashes and polylithologic blocks that include abundant ultramafic nodules. The Imbandina Subsynthem also includes subordinate fine-grained laminated ashes and breccia with travertine overlying an 8 m-thick lava flow. D'Orazio *et al*. (2007, 2008) interpreted these deposits to be the explosive and effusive products (and feeder dikes) of a small carbonatitic volcanic centre (Vallone Toppo di Lupo) that is distinct and younger than the Imbandina Subsynthem. In contrast, Stoppa *et al*. (2008) concluded that no dikes and lavas are present in the Vallone Toppo di Lupo volcanic centre, and that the melilite and carbonatite juvenile lapilli settled into a welded, agglutinated, lapilli ash tuff ring overlying light-brown ash at the top of a large pyroclastic flow unit from the Imbandina vent. Although the focus of our article is not the field origins of the Mt Vulture carbonatites, we concur with the field relationships

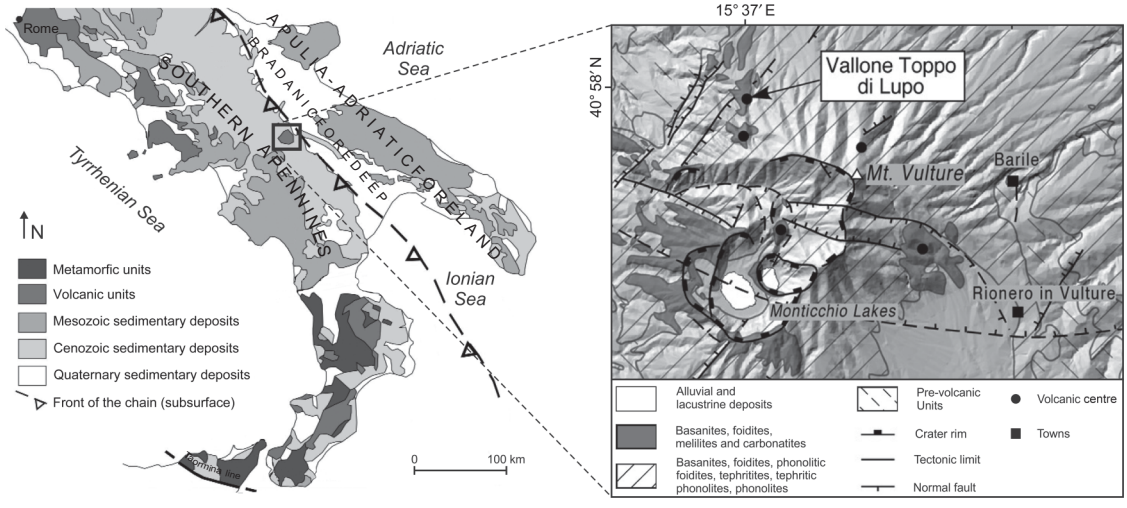

Figure 1. Geological sketch map of the southern Apennines and Mt Vulture area. The carbonatite outcrops and sampling site are shown. Modified after Bonardi *et al*. (2009) and D'Orazio *et al*. (2007).

established by D'Orazio *et al*. (2007) and the identification of two lava flows and a dike in the Vallone Toppo di Lupo volcanic centre.

Sampling and analytical procedures

The rocks studied here are from the Imbandina Subsynthem that was erupted from a small volcanic centre on the northwestern slopes of Mt Vulture at the Vallone Toppo di Lupo locality. The sequence of volcanic rocks comprises lava flows, dikes, and pyroclastic deposits, but this study focuses on the lava flows and dikes. Samples were collected from an upper lava flow ($n = 11$), a lower lava flow ($n = 7$), and a dike ($n = 7$). The two lava flows are massive, light grey in colour, and separated by 5–10 m of pyroclastic material. The upper lava flow is approximately 2.5 m thick and 300 m in length (trending 030–040° with a NW dip of 10–25°). The lower lava flow is slightly thicker and smaller in areal extent (trending 025–030° N with a WNW dip of 35–45°). A massive carbonatite dike, which cross-cuts the upper and lower lava flows, is 60–70 cm thick, trends N–S, and dips 40° W.

Petrographic observations were carried out on thin sections with an optical polarizing microscope. Selected samples were also investigated with an XL-30 Philips LaB_6 environmental scanning microscope (ESEM) (Philips, Eindhoven, The Netherlands) equipped with an energy-dispersive spectrometer (EDS). The abundances of major and trace elements were determined by inductively coupled plasma mass spectrometry (ICP–MS), instrumental neutron activation analysis (INAA), and thermal desorption mass spectrometry (TD–MS) at Activation Laboratories, Ancaster, Ontario, Canada. Average concentration errors are $<\pm5\%$, apart from elements with concentrations ≥10 ppm for which the error is ±5–10%. Multivariate statistical analysis of the elemental data was performed using the Statgraphics Centurion® XVI.I package (StatPoint Technologies Inc., Warrenton, VA, USA).

Petrographic and geochemical data

Figure 2 shows the textures and mineralogical relationships of the carbonatites. Table 1 lists the chemical data of the carbonatites analysed, which are presented separately for the upper lava flow, lower lava flow, and dike. All of the samples studied are hyalo-alvikites (≥50 modal% carbonate), although the upper lava flow, lower lava flow, and dike exhibit significant differences in mineralogy.

Upper lava flow

Samples from the upper lava flow have a porphyritic texture (Figure 2A), with calcite and pyroxene phenocrysts set in a glass-bearing hypidiomorphic matrix. The non-equigranular texture of the hyalo-alvikite is due to the presence of large crystals of clinopyroxene and melilite, phlogopite sheets, amphibole, apatite, and magnetite. Accessory minerals include opaque minerals and small crystals of sagenitic rutile.

Colourless crystals of calcite exhibit polysynthetic twinning and have a prismatic to granular habit. Calcite is also observed in amygdules associated with zeolite (Figure 2B). Porphyroclastic clinopyroxene with a diopsidic composition occurs as large, zoned, homogeneous crystals that exhibit green pleochroism. The amphibole is richterite, and has a prismatic habit that locally forms aggregates around clinopyroxene. Amphibole, apatite microphenocrysts, melilite, phlogopite, magnetite, and Fe-hydroxides are observed as pseudomorphs after clinopyroxene. Large prismatic apatite crystals are present within clinopyroxene. Colourless to yellow melilite crystals have an idiomorphic habit and peg-like structures. Melilite crystal cores are generally surrounded by fine-grained calcite. Sheet-like crystals of phlogopite exhibit signs of ductile deformation, occasionally form aggregates with clinopyroxene and apatite, and contain inclusions of apatite and magnetite. Apatite microcrysts, melilite, clinopyroxene, magnetite, and Fe-hydroxides are pseudomorphs after phlogopite.

Major element data show that CaO is the dominant oxide (36.9–39.0 wt.%), followed by SiO_2 (10.8–16.4 wt.%), Al_2O_3 (3.8–5.8 wt.%), and Fe_2O_3(T) (4.6–6.0 wt.%). Samples from the upper lava flow have CaO/(CaO + MgO + FeO(T) + MnO) ratios of 0.82–0.85, which is consistent with their classification as alvikite. Concentrations of TiO_2 (0.30–0.52 wt.%), MnO (0.39–0.44 wt.%), Na_2O (0.27–0.43 wt.%), and K_2O (0.17–0.27 wt.%) are low. With the exception of sample CS_4, P_2O_5 contents are generally >2 wt.%, which is reflected in the large modal abundance of apatite. Both Sr (7747–9965 ppm) and Ba (5250–7262 ppm) contents are high, and the Sr/Ba ratio varies from 1.0 to 1.8.

The total REE content is high (ΣREE = 1956–2404 ppm), and chondrite-normalized patterns (Figure 3A) exhibit strong light REE (LREE) to heavy REE (HREE) fractionation with $(La/Yb)_N = 76$–89. LREE to middle REE (MREE) and MREE to HREE fractionation expressed as $(La/Sm)_N$ and $(Gd/Yb)_N$, vary from 8.9 to 10.5 and 3.9 to 4.5, respectively. The Eu anomaly (Eu/Eu*) ranges from 0.80 to 0.86. Concentrations of transition metals (Sc = 3–5 ppm, Cr = 9–23 ppm, Co = 10–20 ppm, Cu = 30–50 ppm) and alkali trace elements (Rb = 13–21 ppm, Cs = 1.8–3.5 ppm) are low. In contrast, Th (76–99 ppm), U (39–59 ppm), Pb (73–101 ppm), and V (265–420 ppm) concentrations are high.

Lower lava flow

Lower lava flow samples are porphyritic and contain large phenocrysts and aggregates of calcite. The abundance of primary carbonate is higher in the lower lava flow as

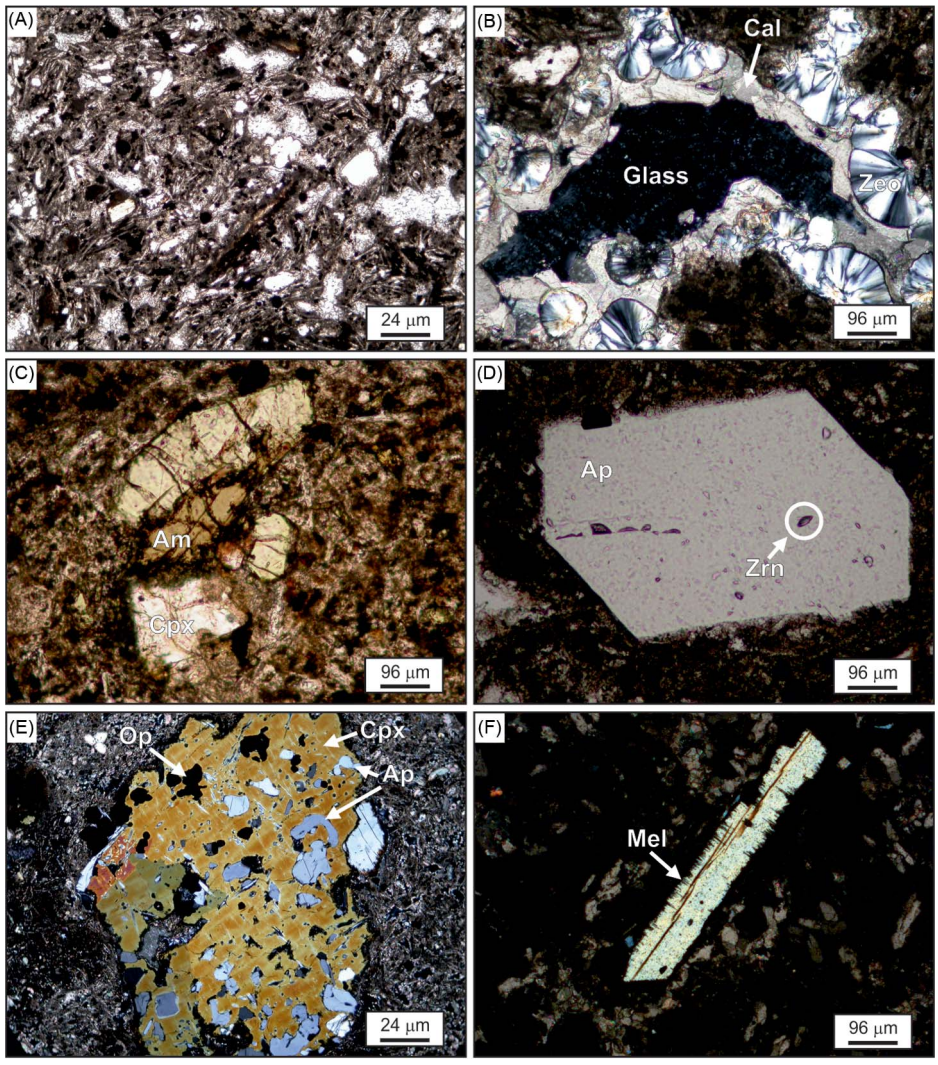

Figure 2. Photomicrographs of massive hyalo-alvikite. PPL, plane-polarized light; CPL, cross-polarized light. (A) Porphyritic texture, PPL, 4X. (B) Amygdules filled by secondary calcite and zeolite, CPL, 10X. (C) Amphibole replaces the clinopyroxene, PPL, 10X. (D) Large euhedral apatite phenocryst with inclusion of zircon, PPL, 10X. (E) Large pecilitic clinopyroxene crystals with inclusions of apatite and opaque minerals, CPL, 10X. (F) Large idiomorphic melilite crystal, CPL, 10X. Symbols were reported for minerals as recommended by Siivola and Schmid (2007).

compared with the upper lava flow. Subordinate amounts of apatite, melilite, acicular phlogopite, clinopyroxene, amphibole, small plagioclase, and opaque minerals also occur as phenocrysts. The amount of clinopyroxene in the lower lava flow is less than that in the upper lava flow. Accessory minerals include opaque minerals and zircon. Calcite, Fe-oxyhydroxides, zeolite, and saussurite are present as secondary phases. Amygdules infilled by calcite, zeolite, and plagioclase are common in the lower lava flow.

The carbonate mineral in the hyalo-alvikite of the lower lava flow is primary calcite. Colourless calcite crystals exhibit polysynthetic twinning and a prismatic to granular habit, whereas matrix calcite has an acicular to prismatic habit. The clinopyroxene has a diopsidic composition and exhibits an idiomorphic and pecilitic habit. Large clinopyroxene xenocrysts of apparently mantle origin are also present. Amphibole may rim the clinopyroxene crystals. Pecilitic crystals include apatite and opaque minerals (Figure 2C), and idiomorphic melilite crystals form peg-like structures (Figure 2D). Sheet-like crystals of phlogopite have a brown to yellow–green colour or are sometimes colourless. Phlogopite occasionally forms aggregates with clinopyroxene and apatite. Primary magmatic plagioclase has sericitic alteration, an idiomorphic habit, and some crystals are replaced by fine-grained Fe-hydroxide. Euhedral and zoned crystals of apatite occur throughout the rocks and abundant subhedral opaque minerals are also present in the matrix. Zircons are found as inclusions in idiomorphic clinopyroxene crystals.

Table 1. Chemical composition of Mt Vulture carbonatites.

	Upper lava flow											Lower lava flow							Dike						
	CS1	CS2	CS3	CS4	CS5	CS6	CS7	CS8	CS9	CS10	CS11	Cl1	Cl2	Cl4	CI5	CI6	CI7	DlC1	DlC2	DlC3	DlC4	DIC5	DIC6	DIC7	
Major elements (wt.%)																									
SiO_2	12.41	15.49	16.08	10.83	12.64	12.44	15.78	13.01	15.67	16.43	11.58	6.70	9.96	8.60	8.53	7.12	9.36	9.12	16.79	16.73	16.28	17.50	17.54	17.79	17.43
Al_2O_3	4.37	5.29	5.34	3.77	4.63	4.47	5.47	4.21	5.05	5.76	4.01	2.61	3.15	3.12	3.05	3.25	3.17	3.23	6.00	5.88	5.75	6.00	5.97	6.01	5.89
Fe_2O_3(T)	5.09	5.69	5.85	4.58	5.19	5.08	5.80	5.16	5.78	5.99	4.76	4.00	3.98	4.13	4.07	4.02	4.17	4.03	5.98	6.17	5.80	6.29	6.12	6.34	6.05
MnO	0.41	0.42	0.43	0.39	0.42	0.41	0.43	0.42	0.43	0.44	0.40	0.47	0.43	0.45	0.45	0.48	0.44	0.43	0.41	0.45	0.43	0.46	0.42	0.45	0.46
MgO	2.09	2.56	2.69	1.96	2.19	2.10	2.68	2.17	2.77	2.89	1.89	0.83	1.43	1.24	1.24	0.94	1.47	1.34	2.81	2.95	2.97	2.93	2.77	3.03	2.96
CaO	38.56	38.22	38.46	37.09	38.52	38.14	36.86	39.02	38.32	38.58	37.54	44.70	40.96	43.33	43.26	45.10	41.24	43.01	37.70	37.87	37.09	38.12	38.10	38.05	37.56
Na_2O	0.27	0.37	0.39	0.28	0.30	0.28	0.43	0.29	0.30	0.43	0.32	0.13	0.35	0.14	0.14	0.21	0.29	0.17	0.62	0.44	0.45	0.44	0.54	0.49	0.46
K_2O	0.24	0.24	0.17	0.22	0.27	0.25	0.18	0.27	0.25	0.21	0.22	0.47	0.27	0.40	0.40	0.39	0.31	0.25	0.51	0.24	0.28	0.23	0.39	0.32	0.27
TiO_2	0.39	0.49	0.51	0.30	0.41	0.39	0.49	0.41	0.52	0.50	0.42	0.16	0.20	0.20	0.20	0.18	0.20	0.20	0.57	0.55	0.49	0.55	0.52	0.55	0.51
P_2O_5	2.08	2.02	2.10	1.85	2.12	2.09	2.18	2.23	2.12	2.14	2.00	2.22	1.79	2.11	2.08	2.34	1.91	2.21	1.99	2.21	2.18	2.25	2.12	2.19	2.31
Total	96.43	96.87	98.00	93.39	96.55	95.61	96.01	98.08	98.22	99.50	96.12	95.92	96.60	96.85	96.42	96.87	96.71	97.50	96.56	94.96	96.07	97.12	97.56	97.20	99.01
Si/Ca	0.21	0.27	0.27	0.19	0.21	0.21	0.28	0.22	0.27	0.28	0.20	0.10	0.16	0.13	0.13	0.10	0.15	0.14	0.29	0.29	0.29	0.30	0.30	0.31	0.30
Trace elements (ppm)																									
Sr	7747	7755	8970	9965	7891	7236	8549	8041	7812	9271	9894	9262	9956	6813	6676	9567	9875	7234	9066	7608	8390	7542	9123	7765	8432
Ba	6888	6224	6117	6459	7262	7008	6032	6750	5250	5250	5400	10,510	11,020	10,040	9786	10,500	10,100	9150	5834	6608	6651	7015	5100	5550	5550
Rb	14	16	16	19	14	13	15	17	17	17	21	19	10	30	32	21	11	34	18	10	7	9	26	8	23
Cs	1.9	3.3	3.4	3.2	2	1.8	3.4	2.2	3.5	3.5	3.5	2.8	1.6	2.6	2.8	3	1.8	2.8	3.9	1.6	3	1.6	4.2	1.4	3.2
Sc	4	5	5	3	3	4	5	4	5	5	3	2	2	2	2	2	2	2	7	6	5	6	6	6	5
Cr	19	18	17	10	15	19	19	21	23	20	9	3	17	15	12	4	15	12	17	27	23	19	15	25	24
Co	12	13	13	10	11	11	13	15	20	19	14	8	7	8	8	13	12	14	14	15	13	15	21	19	21
Cu	30	50	50	30	30	30	40	33	39	39	28	20	20	30	30	20	20	23	43	38	43	40	44	36	41
V	270	383	410	264	282	268	420	283	354	367	265	306	288	314	313	302	290	303	312	466	400	472	293	366	368
Y	70	73	78	65	72	70	76	85	80	80	75	62	61	62	61	71	69	71	70	79	77	80	81	75	85
Zr	74	96	98	58	74	71	99	77	89	95	64	25	37	39	38	28	41	38	98	102	92	99	103	97	94
Pb	73	78	87	79	75	73	84	101	98	99	104	122	108	112	118	141	146	140	88	82	83	82	102	86	100
Th	85.8	85.4	89.1	76.9	85.3	82.2	87.9	86.6	87.1	88	98.7	61.4	62.3	64	63.5	60.4	62.4	62.9	86.5	99.1	85.6	95.1	83.5	90.8	86.5
U	39.6	51.9	57.7	53.8	40	38.7	58.7	42.5	51.2	56.3	58.8	49.5	49.5	54.7	53.7	48.6	51.8	54.9	56.2	60.9	59.6	59.2	61.7	57.6	57.4
Sr/Ba	1.12	1.25	1.47	1.54	1.09	1.03	1.42	1.19	1.49	1.77	1.83	0.88	0.90	0.68	0.68	0.91	0.98	0.79	1.55	1.15	1.26	1.08	1.79	1.40	1.52

(*Continued*)

Table 1. (Continued).

	Upper lava flow											Lower lava flow							Dike						
	CS1	CS2	CS3	CS4	CS5	CS6	CS7	CS8	CS9	CS10	CS11	Cl1	Cl2	Cl4	Cl5	Cl6	Cl7	DlC1	DlC2	DlC3	DlC4	DlC5	DlC6	DlC7	
Rare earth elements (ppm)																									
La	605	598	615	578	628	594	584	699	621	590	630	734	661	693	695	747	681	737	597	688	573	649	608	584	626
Ce	980	985	996	925	975	961	945	1150	1040	990	1030	1110	1020	1060	1060	1150	1080	1140	961	1080	928	1050	1010	960	1040
Pr	93.6	92.9	94.3	87.7	95.1	89.9	92.6	105	96.1	90.9	94	102	92.4	98	95.8	99.9	95.3	101	92.2	106	90.4	101	95	88.9	96.3
Nd	293	294	306	273	307	290	298	331	307	288	298	300	276	288	291	298	288	307	295	344	291	321	300	284	306
Sm	39.2	40.4	41.5	34.8	40.1	38.4	41.5	43	41	38	39	36.2	34.6	35.5	35.5	35	35	37	40.7	45.5	40.1	42.7	40	37	41
Eu	8.52	8.67	9.12	7.77	8.85	8.36	9.29	9.81	9.33	8.79	8.75	8.08	7.51	7.85	7.68	7.94	7.95	8.23	8.91	10.1	9.04	9.48	9.15	8.73	9.2
Gd	24.9	25.4	26.3	22.2	24.7	24.3	26.7	32	30	29	29	23.2	21	21.7	24.2	25	25	27	28	31.5	28.4	29.2	29	28	30
Tb	2.8	2.8	3	2.6	2.9	2.7	3.3	2.6	2.6	2.7	2.8	2.6	2.4	2.5	2.6	3.1	3	3.2	3	3.3	3.3	3.3	16	15	16
Dy	13	13.8	14.5	12.3	14.1	12.9	15.5	13.6	14.1	15	12.1	11.7	11.4	11.8	11.9	15.3	14.9	15.5	14.2	16.3	15	15.3	16	15.3	16.2
Ho	2.2	2.4	2.4	2.1	2.4	2.2	2.7	3	2.8	2.7	2.7	2	1.9	2	2	2.3	2.3	2.4	2.5	2.8	2.6	2.6	2.8	2.6	2.8
Er	6	6.3	6.8	5.5	6.2	6	7.2	8	7	7	7	5.5	5.3	5.5	5.7	6	6	6	6.5	7.1	7.4	6.9	7	7	7
Tm	0.82	0.87	0.91	0.74	0.83	0.8	0.96	1	0.9	0.9	0.9	0.75	0.73	0.73	0.75	0.8	0.8	0.8	0.88	1.02	0.95	0.94	0.9	0.9	1
Yb	4.7	5	5.3	4.4	5	4.8	5.6	5.8	5.4	5.2	5.2	4.5	4.3	4.5	4.4	4.6	4.6	4.8	5.1	5.7	5.4	5.5	5.5	4.9	5.6
Lu	0.67	0.71	0.75	0.64	0.71	0.67	0.77	0.67	0.73	0.77	0.68	0.62	0.59	0.66	0.62	0.6	0.6	0.6	0.71	0.82	0.77	0.77	0.7	0.7	0.7
ΣREE	2074.41	2076.25	2121.88	1956.75	2110.89	2036.03	2033.12	2404.48	2177.96	2068.96	2160.13	2341.15	2139.13	2231.74	2237.15	2395.54	2244.45	2390.53	2055.7	2342.14	1995.36	2237.69	2140.05	2037.03	2197.8
$(La/Yb)_N$	86.98	80.82	78.41	88.77	84.87	83.62	70.47	81.44	77.71	76.67	81.87	110.22	103.88	104.07	106.74	109.74	100.04	103.76	79.10	81.56	71.70	79.74	74.70	80.54	75.54
$(La/Sm)_N$	9.71	9.32	9.33	10.45	9.86	9.74	8.86	10.23	9.53	9.77	10.17	12.76	12.02	12.29	12.32	13.43	12.25	12.54	9.23	9.52	8.99	9.57	9.57	9.93	9.61
$(Gd/Yb)_N$	4.29	4.12	4.02	4.09	4.00	4.10	3.86	4.47	4.50	4.52	4.52	4.18	3.96	3.91	4.46	4.40	4.40	4.56	4.45	4.48	4.26	4.30	4.27	4.63	4.34
Eu/Eu*	0.83	0.83	0.84	0.85	0.86	0.84	0.85	0.81	0.81	0.81	0.80	0.85	0.85	0.86	0.80	0.82	0.82	0.80	0.81	0.82	0.82	0.82	0.82	0.83	0.80

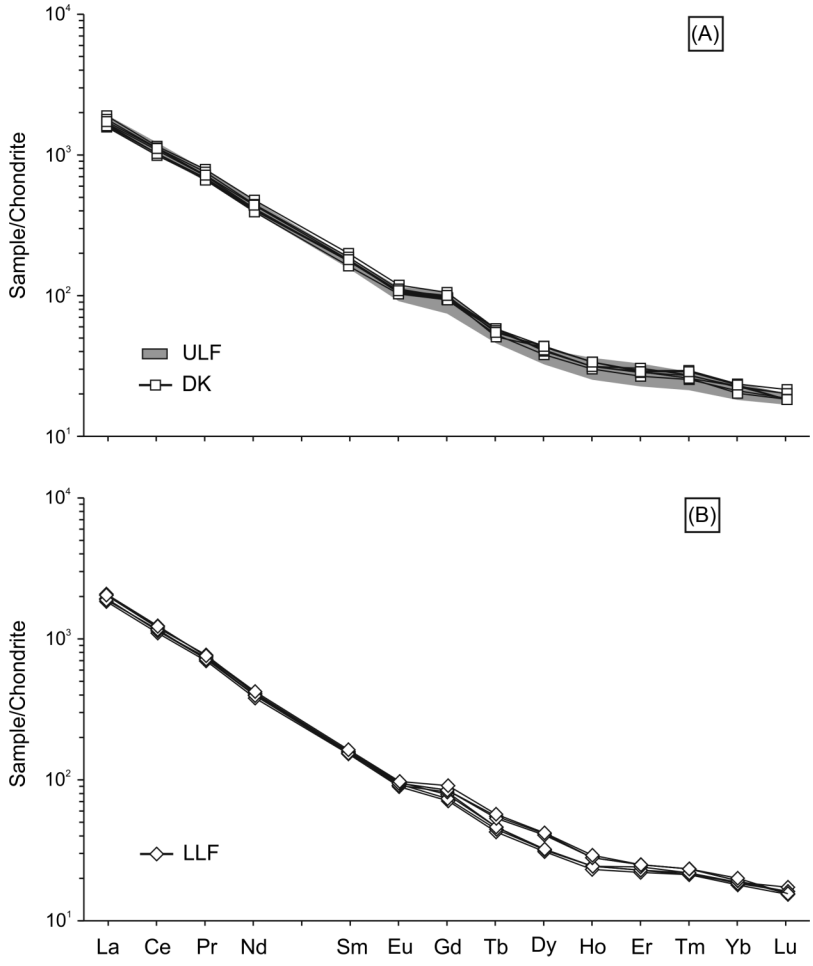

Figure 3. Chondrite-normalized rare earth element (REE) patterns; chondrite values are from Evensen *et al*. (1978). See text for further details.

The higher abundance of calcite in the lower lava flow relative to the upper lava flow is also evident from the former's higher CaO (41.0–45.1 wt.%), lower concentrations of other major elements (SiO_2 = 6.7–10.0 wt.%, Al_2O_3 = 2.6–3.3 wt.%, Fe_2O_3(T) = 4.0–4.2 wt.%), and higher CaO/(CaO + MgO + FeO(T) + MnO) ratios of 0.88–0.90. P_2O_5 contents vary from 1.8 to 2.3 wt.%, whereas the concentrations of TiO_2 (0.16–0.20 wt.%), MnO (0.43–0.48 wt.%), Na_2O (0.13–0.35 wt.%), and K_2O (0.25–0.47 wt.%) are low. A high Ba content (9150–11,020 ppm) is associated with a higher abundance of zeolite in the lower lava flow as compared with the upper lava flow, which is also evident from low Sr/Ba ratios of 0.68–0.98 and ESEM-EDS results.

Chondrite-normalized REE patterns of the lower lava flow samples (Figure 3B) have higher LREE/HREE ratios ($(La/Yb)_N$ = 100–110) and LREE/MREE fractionations ($(La/Sm)_N$ = 12.0–13.4) than the upper lava flow samples. In contrast, the total amounts of REE (ΣREE = 2139–2395 ppm), MREE/HREE fractionation ($(Gd/Yb)_N$ = 4.0–4.6), and Eu anomaly (Eu/Eu^* = 0.80–0.86) are similar for both lava flows and are apparently unaffected by their mineralogical differences. As is the case for the upper lava flow, the lower lava flow samples have low concentrations of transition metals (Sc = 2 ppm, Cr = 3–17 ppm, Co = 7–14 ppm, Cu = 20–30 ppm) and alkali trace elements (Rb = 10–34 ppm, Cs = 1.6–2.8 ppm), and high concentrations of actinides (Th = 60–64 ppm, U = 48–55 ppm, Pb = 108–146 ppm, and V = 288–315 ppm).

Dike

The dike samples have porphyritic and intersertal textures, and a phenocryst assemblage similar to those of the upper lava flow. The dike matrix comprises calcite, clinopyroxene, orthopyroxene, phlogopite, plagioclase, amphibole, and small acicular crystals of accessory apatite and magnetite. Secondary calcite and subordinate Ba-zeolite form radiating aggregates in amygdules.

Primary calcite in the dike has either a prismatic or granular habit. Primary diopsidic clinopyroxene crystals

are often twinned and zoned, and some crystals are pecilitic and contain numerous large apatite inclusions. Hastingsitic amphibole exhibits a prismatic habit and sometimes forms crystal aggregates. The amphibole may occur as either single crystals or an overgrowth on clinopyroxene (Figure 2E). Phlogopite is brown to yellow–green or sometimes colourless, contains apatite inclusions, and occasionally forms aggregates with clinopyroxene and apatite. Plagioclase crystals are small subhedral prisms and exhibit deformation twinning. Apatite occurs as zoned euhedral crystals, and apatite microphenocrysts are found within clinopyroxene and phlogopite. Zircon inclusions occur in apatite (Figure 2F), whereas opaque mineral inclusions are found within amphibole.

Calcium is the dominant major element in the dike (CaO = 37.1–38.1 wt.%), with progressively lower concentrations of SiO_2 (16.3–17.8 wt.%), Al_2O_3 (5.8–6.0 wt.%), and Fe_2O_3(T) (5.8–6.3 wt.%). The CaO/(CaO + MgO + FeO(T) + MnO) ratio for the dike samples is 0.81. Concentrations of TiO_2 (0.49–0.57 wt.%), MnO (0.41–0.46 wt.%), Na_2O (0.44–0.62 wt.%), and K_2O (0.23–0.51 wt.%) in the dike are low. P_2O_5 contents vary from 2.0 to 2.3 wt.%. Sr and Ba abundances in the dike are high (Sr = 7765–9123 ppm, Ba = 5100–7015 ppm) and the Sr/Ba ratio varies from 1.1 to 1.8, which is similar to the upper lava flow.

The concentrations of REE in the dike are also similar to those of the upper lava flow. The total amount of REE varies from 1995 to 2342 ppm. Chondrite-normalized REE patterns are characterized by significant LREE/HREE fractionation with $(La/Yb)_N$ = 71–82 (Figure 3A). $(La/Sm)_N$ and $(Gd/Yb)_N$ ratios vary from 9.0 to 19.9 and 4.3 to 4.6, respectively. The Eu/Eu* anomaly ranges from 0.80 to 0.83. The concentrations of transition metals (Sc = 5–7 ppm, Cr = 15–27 ppm, Co = 13–21 ppm, Cu = 36–44 ppm) and alkali trace elements (Rb = 7–26 ppm, Cs = 1.4–3.9 ppm) are low in the dike, but concentrations of Th (83–99 ppm), U (56–62 ppm), Pb (82–102 ppm), and V (293–472 ppm) are high.

REE characteristics and processes affecting their distribution in the carbonatites

The high $(La/Yb)_N$ values clearly show that the Mt Vulture carbonatites are LREE-enriched, which is a common feature of carbonatites worldwide and is often related to Ba and Sr enrichment (e.g. Tucker *et al*. 2012, and references therein). The Mt Vulture carbonatites have Sr contents that are similar to those of average calcio-carbonatites, whereas the higher Ba contents of the Mt Vulture carbonatites, like those of the lower lava flow, are comparable to those of the Bayan Obo REE ore (Inner Mongolia, China) (Figure 4A). However, the LREE grade of the Mt Vulture carbonatites is approximately one order of magnitude lower than that of the Bayan Obo deposit and similar to that of average calcio-carbonatite (Figures 4B and C). This is consistent with the absence of REE-minerals in the Mt Vulture carbonatites. To evaluate the relationships between mineralogy and major and trace elements, we conducted R-mode factor analysis using principal component analysis after Varimax rotation. This analysis was performed on a standardized correlation matrix, with equal weighting for all variables, which makes it possible to convert the principal component vectors into factors. Subsequently, the factor loadings (Table 2) were considered.

Three factors explain 81.3% of the total variance of the data set considered. The first factor (F1: variance = 55.0%) shows a strong positive weighting for SiO_2 and many trace elements, including the transition metals (Sc, Cr, Co, and Cu), Zr, Yb, and Th. CaO, Ba, La, and Pb show a significant and negative weighting for this factor. In the carbonatites, transition metals are hosted by pyroxene, phlogopite, and amphibole (e.g. Stoppa and Wolley 1997; Stoppa *et al*. 2005; Reguir *et al*. 2009), whereas zircon controls Zr, Yb, and Th (e.g. Harley and Kelly 2007; Seifert *et al*. 2012). Chen and Simonetti (2012) showed that Ba and LREE with concentrations >100 ppm are the most abundant trace elements in calcite from the Oka carbonatite complex (Canada) and that the Pb contents are also not negligible. In addition, the association between Ba and CaO for F1 may a function of the occurrence of Ba-zeolite and secondary calcite in amygdules. However, it should be noted that although LREE enrichment varies significantly in calcite samples from the Oka carbonatite (e.g. average La = 286 ± 160 ppm, n = 24), the carbonate always displays steeply negative chondrite-normalized distribution patterns (Chen and Simonetti 2012). Thus, F1 represents the competing effects between silicate minerals and calcite in controlling the distribution of trace elements.

The second factor (F2) explains 17.1% of the total variance of the data set. For F2, only P_2O_5, ΣREE, and La have significant and positive weightings. Apatite is an important phase in controlling REE concentrations in carbonatites, particularly with respect to the LREE. For example, Chen and Simonetti (2012) showed that a single apatite crystal can contain up to approximately 45,000 ppm of ΣREE and 14,000 ppm of La. Apatite is a common mineral in the Mt Vulture carbonatites. F2 is thus related to the role of apatite in distributing REE and, in particular, the LREE in the carbonatites.

The third factor (F3: variance = 9.2%) is characterized only by significant and positive weightings for V and U, which share a common mineralogical control as hydrated vanadates. These minerals, such as carnotite ($K_2(UO_2)_2V_2O_8 \cdot 3(H_2O)$) and tyuyamunite ($Ca(UO_2)_2V_2O_8 \cdot 5–8(H_2O)$), are secondary in origin and

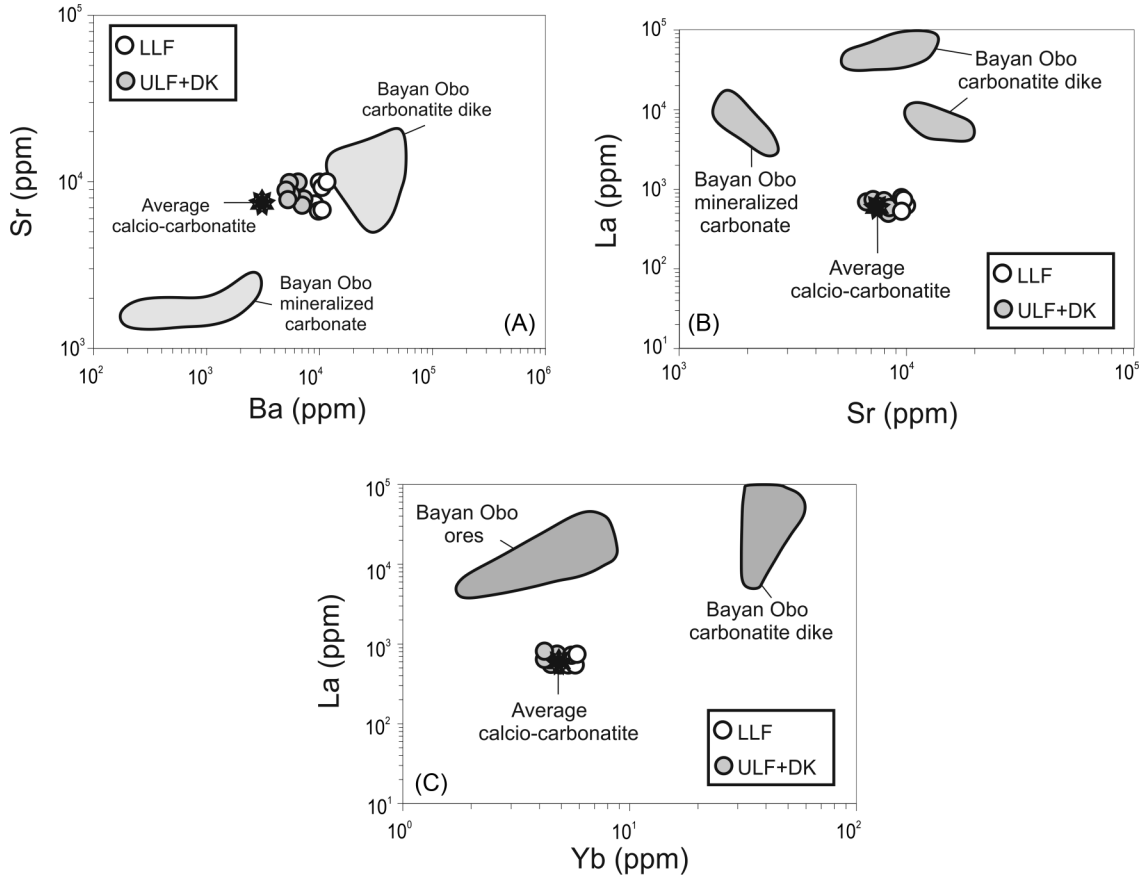

Figure 4. Binary plots (after Tucker *et al*. 2012) illustrating the magnitude and significance of Sr, Ba, and La enrichment in the Mt Vulture carbonatites. Average calcio-carbonatite data are from Woolley and Kempe (1989).

Table 2. R-mode factor analysis results.

Elements	Factor 1	Factor 2	Factor 3
SiO_2	0.86		
CaO	−0.86		
P_2O_5		0.76	
Sc	0.82		
V			0.72
Cr	0.61		
Co	0.62		
Cu	0.73		
Sr			
Zr	0.91		
Ba	−0.89		
La	−0.61	0.75	
Yb	0.86		
ΣREE		0.86	
Pb	−0.63		
Th	0.94		
U			0.88
Var.%	55	17.1	9.2

Notes: Numbers are weights of the variables in the extracted factors. Variables having weights less than 0.60 are omitted.

generally associated with sedimentary rocks (e.g. Fayek *et al*. 2011). However, Wenrich *et al*. (1982) discovered a Cs-rich analogue of carnotite (i.e. margaritasite) as disseminated pore fillings and phenocryst relict linings within a rhyodacitic tuff breccia. Although we did not find uranium vanadates in the Mt Vulture carbonatites, perhaps due to their very low abundance, it is possible that F3 may reveal their presence.

This multivariate analysis suggests that the REE are hosted in several minerals. Given that apatite occurs as an accessory mineral and the calcite abundance is ≥50 modal%, we can broadly assume that CaO contents are representative of calcite abundance. Similarly, we can assume that SiO_2 and P_2O_5 contents are indicative of silicate mineral and apatite abundances, respectively. Using these assumptions, it is then possible to explore whether these parameters control $(La/Yb)_N$, $(La/Sm)_N$, $(Gd/Yb)_N$, and Eu anomalies (Figure 5). SiO_2 contents and silicate mineral abundance are generally inversely correlated with $(La/Yb)_N$ and $(La/Sm)_N$ ratios as represented by F1. Increasing CaO and calcite abundance is associated with an increase in both $(La/Yb)_N$ and $(La/Sm)_N$,

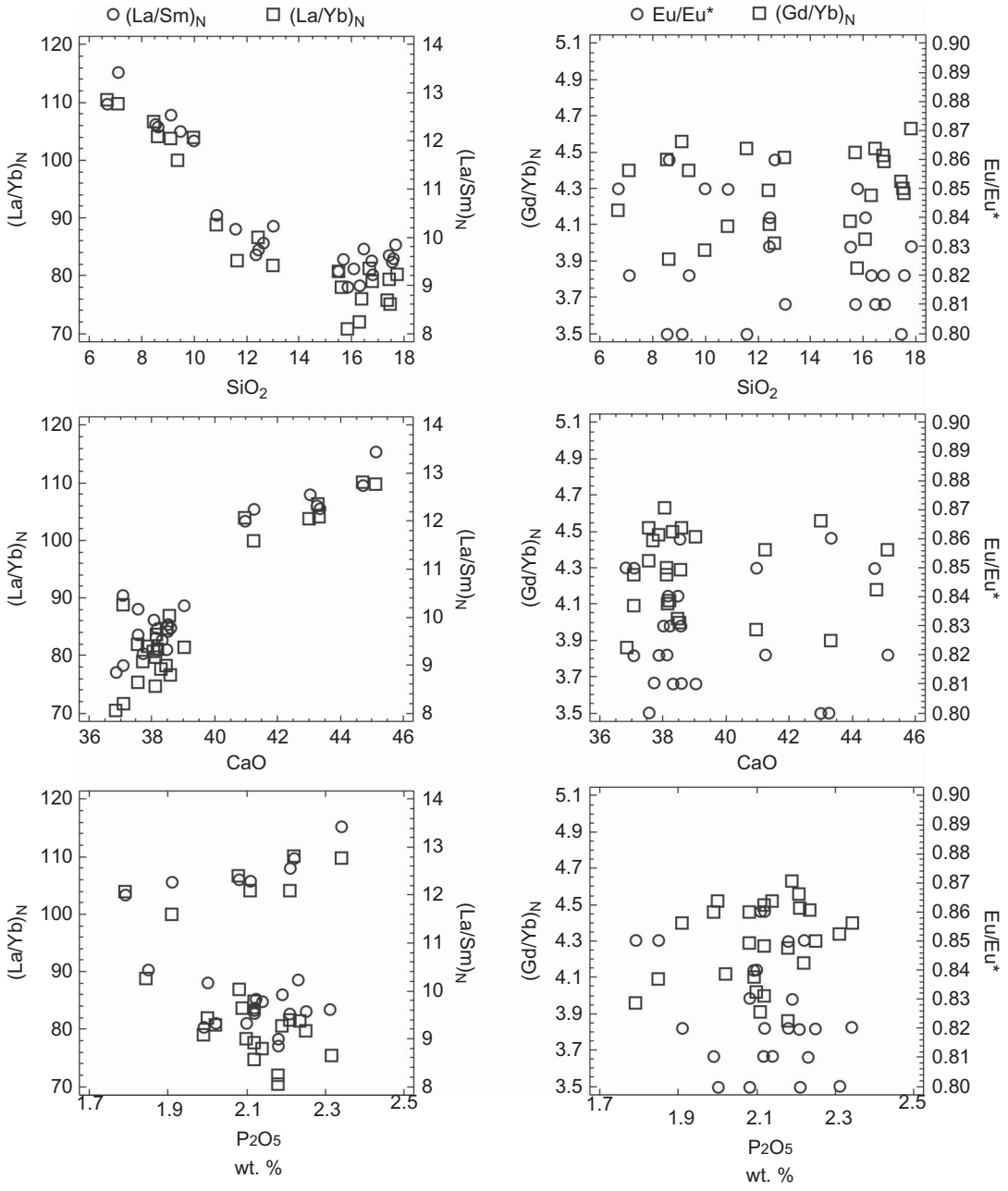

Figure 5. Binary plots showing the SiO_2, CaO, and P_2O_5 influence on the REE fractionation indexes. See text for further details.

which is also represented by F1. Plots of P_2O_5 *versus* $(La/Yb)_N$ and $(La/Sm)_N$ show a scattered distribution of data, suggesting that apatite exerts a minor role, if any, in controlling LREE/HREE and LREE/MREE fractionations in the Mt Vulture carbonatites. Similarly, SiO_2, CaO, and P_2O_5 when plotted against $(Gd/Yb)_N$ and Eu/Eu^* show no coherent trends. As such, the Eu anomaly and MREE/LREE fractionations are not a simple function of the relative abundance of silicate minerals and calcite or the modal proportion of apatite.

Conclusions

Mineralogical and chemical differences characterize the Mt Vulture carbonatites sampled from the upper lava flow (and dike) and the lower lava flow. The latter is enriched in calcite, Ba, and LREE and has steeper chondrite-normalized REE patterns with $(La/Yb)_N > 100$. In general, the REE grade of the Mt Vulture carbonatites is comparable to that of average calcio-carbonatite. A statistical evaluation of the inter-elemental relationships of the carbonatites indicates that most of the compositional

variance mirrors the relative abundances of silicate minerals and calcite, with the silicate phases controlling transition metal, Th, Zr, and HREE abundances, whereas LREE abundances are controlled by calcite and apatite. SiO_2 and CaO contents reflect the relative abundances of silicate minerals and calcite, respectively, and also REE fractionation. Increasing SiO_2 is associated with decreasing $(La/Yb)_N$ and $(La/Sm)_N$, and less steep chondrite-normalized REE patterns. Higher carbonate contents are correlated with increases in $(La/Yb)_N$ and $(La/Sm)_N$ ratios, which results in steeper chondrite-normalized REE patterns. Thus, a striking correlation exists between Si/Ca and $(La/Yb)_N$ ($r = -0.94$) and $(La/Sm)_N$ ($r = -0.92$) in the Mt Vulture carbonatites. Furthermore, Si/Ca ratios do not correlate with Eu anomaly or MREE/HREE fractionation ($r_{Eu/Eu^*} = -0.21$, $r_{(Gd/Yb)N} = 0.22$). This requires that Eu/Eu^* and $(Gd/Yb)_N$ are controlled by a range of factors, and not simply by the ratio of silicate minerals to calcite. Although apatite is an important REE host, its minor abundances in the carbonatites as compared with silicate minerals and calcite means that it has a negligible effect on inter-REE fractionations.

Acknowledgements

The authors are grateful to Professors S. Critelli and R.V. Ingersoll for their helpful suggestions and precious support. They also thank A. Laurita, CIGAS – Centro Interdipartimentale Grandi Attrezzature Scientifiche, University of Basilicata, for ESEM-EDS facilities, and Dr R. Santochirico and Dr L. Lovallo for their support during sampling and field activities. The research was financially supported by G. Mongelli, M. Paternoster, and G. Rizzo grants (RIL 2009).

References

Beccaluva, L., Coltorti, M., Di Girolamo, P., Melluso, L., Milani, L., Morra, V., and Siena, F., 2002, Petrogenesis and evolution of Mt Vulture alkaline volcanism (southern Italy): Mineralogy and Petrology, v. 74, p. 277–297.

Bell, K., 1998, Radiogenic isotope constraints on relationships between carbonatites and associated silicate rocks: a brief review: Journal of Petrology, v. 39, p. 1987–1996.

Bonardi, G., Ciarcia, S., Di Nocera, S., Matano, F., Srosso, I., and Torre, M., 2009, Carta delle principali unità cinematiche dell'Appennino meridionale. Nota illustrativa: Ital. J. Geosci, v. 128, p. 47–60.

Büettner, A., Principe, C., Villa, I.M., and Brocchini, D., 2006, Geocronologia ^{39}Ar–^{40}Ar del Monte Vulture, *in* Principe, C., ed., La geologia del Monte Vulture: Regione Basilicata: Lavello, Italy, Dipartimento Ambiente, Territorio e Politiche della Sostenibilità. Grafiche Finiguerra, p. 73–86.

Caracausi, A., Martelli, M., Nuccio, P.M., Paternoster, M., and Stuart, F.M., 2013, Active degassing of mantle-derived fluid: A geochemical study along the Vulture line, southern Apennines (Italy): Journal of Volcanology and Geothermal Research, v. 253, p. 65–74.

Chen, W., and Simonetti, A., 2012, In-situ determination of major and trace elements in calcite and apatite, and U–Pb ages of apatite from the Oka carbonatite complex: Insights into a complex crystallization history: Chemical geology (in press), doi: 10.1016/j.chemgeo.2012.04.022.

De Fino, M., La Volpe, L., Peccerillo, A., Piccarreta, G., and Poli, G., 1986, Petrogenesis of Monte Vulture volcano (Italy): Inferences from mineral chemistry, major and trace element data: Contributions to Mineralogy and Petrology, v. 92, p. 135–145.

Doglioni, C., Mongelli, F., and Pieri, P., 1994, The Puglia uplift (SE Italy): An anomaly in the foreland of the Apenninic subduction due to buckling of a thick continental lithosphere: Tectonics, v. 13, p. 1309–1321.

Downes, H., Kostoula, T., Jones, A.P., Beard, A.D., Thirlwall, M.F., and Bodinier, J.L., 2002, Geochemistry and Sr–Nd isotopic compositions of mantle xenoliths from the Monte Vulture carbonatite-melilitite volcano, central southern Italy: Contributions to Mineralogy and Petrology, v. 144, p. 78–92.

D'Orazio, M., Innocenti, F., Tonarini, S., and Doglioni, C., 2007, Carbonatites in a subduction system: The Pleistocene alvikites from Mt Vulture (southern Italy): Lithos, v. 98, p. 313–334.

D'Orazio, M., Innocenti, F., Tonarini, S., and Doglioni, C., 2008, Reply to the discussion of: "Carbonatites in a subduction system: The Pleistocene alvikites from Mt Vulture (Southern Italy)" (Lithos 98, 313–334) by F. Stoppa, C. Principe and P. Giannandrea: Lithos, v. 103, p. 557–561.

Evensen, M.N., Hamilton, P.J., and O'Nions, R.K., 1978, Rare-earth abundances in chondritic meteorites: Geochimica et Cosmochimica Acta, v. 42, p. 1199–1212.

Fayek, M., Horita, J., and Ripley, E.M., 2011, The oxygen isotopic composition of uranium minerals: A review: Ore Geology Reviews, v. 41, p. 1–21.

Giannandrea, P., La Volpe, L., Principe, C., and Schiattarella, M., 2004, Carta geologica del Mt Vulture a 1:25.000: Litografia Artistica Cartografica Srl., Firenze.

Giannandrea, P., Principe, C., La Volpe, L., and Schiattarella, M., 2006a, Unità stratigrafiche a limiti inconformi e storia evolutiva del vulcano medio-pleistocenico di Monte Vulture (Appennino meridionale, Italia): Bollettino Societa Geologica Italiana, v. 125, p. 67–92.

Giannandrea, P., Principe, C., La Volpe, L., and Schiattarella, M., 2006b, Note illustrative alla nuova carta geologica alla scala 1: 25.000 del Monte Vulture – The new geological map 1:25.000 of Monte vulture volcano, *in* Principe, C., ed., Geologia del Monte Vulture: Finiguerra, Lavello, Monografia geologica, Regione Basilicata Dipartimento Ambiente e Territorio, p. 25–49.

Harley, S.L., and Kelly, N.M., 2007, The impact of zircon–garnet REE distribution data on the interpretation of zircon U–Pb ages in complex high-grade terrains: An example from the Rauer Islands, East Antarctica: Chemical Geology, v. 241, p. 62–87.

Harmer, R.E., and Gitiins, J., 1998, The case for primary, mantle-derived carbonatite magma: Journal of Petrology, v. 39, p. 1895–1903.

Jones, A.P., Kostoula, T., Stoppa, F., and Woolley, A.R., 2000, Petrography and mineral chemistry of mantle xenoliths in a carbonate-rich melilititic tuff from Mt Vulture volcano, southern Italy: Mineralogical Magazine, v. 64, p. 593–613.

Kjarsgaard, B.A., and Hamilton, D.L., 1989, The genesis of carbonatites by immiscibility, *in* Bell, K., ed., Carbonatites: Genesis and evolution: London, Unwin Hyman, p. 388–404.

Koster van Groos, A.F., and Wyllie, P.J., 1963, Experimental data bearing on the role of liquid immiscibility in the genesis of carbonatites: Nature, v. 199, p. 801–802.

Le Maitre, R.W., 2002, Igneous rocks: A classification and glossary of terms: Cambridge, UK, Cambridge University Press.

Lee, W.J., and Wyllie, P.J., 1994, Experimental data bearing on liquid immiscibility, crystal fractionation, and the origin of calciocarbonatites and natrocarbonatites: International Geology Review, v. 36, p. 797–819.

Ray, J.S., Ramesh, R., Pande, R.K., Trivedi, J.R., Shukla, P.N., and Patel, P.P., 2000, Isotope and rare earth element chemistry of carbonatite ± alkaline complexes of Deccan volcanic province: Implications to magmatic and alteration processes: Journal of Asian Earth Sciences, v. 18, p. 177–194.

Reguir, E.P., Chakhmouradian, A.R., Halden, N.M., Malkovets, V.G., and Yang, P., 2009, Major- and trace-element compositional variation of phlogopite from kimberlites and carbonatites as a petrogenetic indicator: Lithos, v. 112S, p. 372–384.

Rosatelli, G., Wall, F., and Stoppa, F., 2007, Calcio-carbonatite melts and metasomatism in the mantle beneath Mt Vulture (southern Italy): Lithos, v. 99, p. 229–248.

Seifert, W., Förster, H.J., Rhede, D., Tietz, O., and Ulrych, J., 2012, Mineral inclusions in placer zircon from the Ohře (Eger) Graben: New data on "strontiopyrochlore: Mineralogy and Petrology, v. 106, p. 39–53.

Serri, G., Innocenti, F., and Manetti, P., 2001, Magmatism from Mesozoic to Present: petrogenesis, time-space distribution and geodynamic implications, *in* Vai, G.B., and Martini, I.P., eds., Anatomy of an orogen: The Apennines and adjacent Mediterranean basins: Dordrecht, Kluwer Academic Publishers, p. 77–103.

Siivola, J., and Schmid, R., 2007, List of mineral abbreviations: Recommendations by the subcommission on the systematics of metamorphic rocks, 12, Web version 01.02.07.

Srivastava, R.K., Heaman, L.M., Sinha, A.K., and Sun, S.H., 2005, Emplacement age and isotope geochemistry of Sung Valley alkaline-carbonatite complex, Shillong Plateau, northeastern India: Implications for primary carbonate melt and genesis of the associated silicate rocks: Lithos, v. 81, p. 33–54.

Stoppa, F., and Principe, C., 1997, Eruption style and petrology of a new carbonatitic suite from the Mt Vulture, southern Italy: The Monticchio lakes Formation: Journal of Volcanology and Geothermal Research, v. 78, p. 251–265.

Stoppa, F., Principe, C., and Giannandrea, P., 2008, Comments on: Carbonatites in a subduction system: The Pleistocene alvikites from Mt Vulture (southern Italy) by d'Orazio et al., (2007): Lithos, v. 103, p. 550–556.

Stoppa, F., Rosatelli, G., Wall, F., and Jeffries, T., 2005, Geochemistry of carbonatite-silicate pairs in nature: A case history from Central Italy: Lithos, v. 85, p. 26–47.

Stoppa, F., and Wolley, A.R., 1997, The Italian carbonatites: Field occurrence, petrology and regional significance: Mineralogy and Petrology, v. 59, p. 43–67.

Sweeney, R., 1994, Carbonatite melt compositions in the earth mantle: Earth and Planetary Science Letters, v. 128, p. 259–270.

Tucker, R.D., Belkin, H.E., Schulz, K.J., Peters, S.G., Horton, F., Buttleman, K., and Scott, E.R., 2012, A major light rare-earth element (Lree) resource in the Khanneshin carbonatite Complex, southern Afghanistan: Economic Geology: v. 207, p. 197–205.

Veksler, I.V., Nielsen, T.F.D., and Sokolov, S.V., 1998, Mineralogy of crystallized melt inclusions from Gardiner and Kovdor ultramafic alkaline complexes: Implications for carbonatite genesis: Journal of Petrology, v. 39, p. 2015–2031.

Wenrich, K.J., Modreski, P.J., Zielinski, R.A., and Seeley, J.L., 1982, Margaritasite: A new mineral of hydrothermal origin from the Peña Blanca uranium district, Mexico: American Mineralogy, v. 67, p. 1273–1289.

Woolley, A.R., and Kempe, D.R.C., 1989, Carbonatites: Nomenclature, average chemical compositions, and element distributions, *in* Bell, K., ed., Carbonatites, genesis and evolution: London, Unwin Hyman, p. 1–14.

Xu, C., Wang, L., Song, W., and Vuet, M., 2010, Carbonatites in China: A review for genesis and mineralization: Geoscience Frontiers, v. 1, p. 105–114.